Multiscale and Multidisciplinary Modeling, Experiments and Design
https://doi.org/10.1007/s41939-024-00472-w

ORIGINAL PAPER

Development of a hybrid material with auxetic phase

Maciej Zawistowski[1] · **Arkadiusz Poteralski**[1]

Received: 7 February 2024 / Accepted: 4 May 2024
© The Author(s) 2024

Abstract
Hybrid multiphase materials exhibit a wide range of desirable properties, which may be tailored to the needs of their user or application. Modern solutions often use advanced smart materials with specific properties, which in some cases allow the development of devices previously impossible to manufacture due to restrictions of conventional materials. There is ongoing research on multiphase materials composed of phases with differing Poisson's ratios, which have increased elastic modulus compared to their respective monophase components. Precise analysis of multiphase materials composed of periodic microstructures is possible with the use of multiscale modeling methods and numerical homogenization of individual phases' geometric structures into homogenous materials retaining the properties of their representative volume elements. Auxetic materials behavior under loading differs from conventional materials. Their Poisson's ratio value is negative, which means that when they are uniaxially stretched they both elongate and expand laterally, and while uniaxially compressed they both shorten and shrink laterally. While seemingly changing volume, their density remains constant in microscale. Deformation causes the gaps in auxetics patterned structure to change shape and size, but the actual material of the structure remains unchanged. This paper presents the results of development of a multiphase hybrid material with auxetic phase, in two variants. First, with the goal of maximization of the material's elastic modulus. Second, to obtain a zero-value effective Poisson's ratio. Different patterns of phases distribution in the material were analyzed. A few different auxetic structures were taken into consideration. Optimization utilized numerical simulation based on finite element method.

Keywords Auxetic materials · Finite element method · Multiphase material · Multiscale modeling

1 Introduction

Modern material engineering allows for development of hybrid materials and multimaterials, consisting of various phases of different materials in specific shapes and scales. By combining two or more conventional materials it is possible to obtain hybrid materials with specific sets of properties, often very different than those of their components. This allows for development of new advanced devices, which previously might have been impossible to manufacture due to restrictions of conventional materials. It also allows to tailor material properties to a specific application, for optimal design. In this approach the word "material" is used as an umbrella term for both its original meaning and more broadly, like for example galvanized steel—indivisible material from which a given object is manufactured or a representative of a given microstructure with specific set of properties (Kromm et al. 2002; Ashby and Bréchet 2003). In scope of this paper the term "material" is used in its conventional meaning in regard to bulk material and additionally as phases with specific sets of material properties obtained via multiscale modeling of specific periodic microstructures. By "hybrid material" the authors of this work refer to the material obtained by combining two phases with different periodic microstructures mentioned above.

Auxetic materials, in contrast to conventional materials, behave counterintuitively when mechanically loaded. Uniaxial tension causes them to elongate and widen, and uniaxial compression – to shorten and shrink, seemingly changing volume. This behavior stems from specific geometries of their internal structures, which are similar to lattice structures with internal gaps. Mechanical loading causes beams of those structures to move about each other, causing the gaps

✉ Maciej Zawistowski
maciej.zawistowski@polsl.pl

Arkadiusz Poteralski
arkadiusz.poteralski@polsl.pl

[1] Department of Computational Mechanics and Engineering, Faculty of Mechanical Engineering, Silesian University of Technology, Konarskiego 18A, 44-100 Gliwice, Poland

Published online: 20 May 2024

to enlarge in case of tension or to shrink in case of compression. Density and total volume of the bulk material remains the same during elastic deformation, even though auxetics seemingly change their volume. The term "auxetic" comes from Greek αὐξητικός (transliteration: *auxetikos)*, meaning "that which tends to increase". It was introduced in 1991 by Evans (Evans 1991) and is used to refer to materials with negative Poisson's ratio.

Material parameter which describes the extent of auxetic effect is the Poisson's ratio. In isotropic conventional materials its value is in the range of 0 to 0.5 (0.3 for steel) and in auxetics its values are negative, up to − 1.0 for isotropic auxetics. The value of Poisson's ratio, so also the extent of auxetic effect, is mostly dependent on geometry of internal structure of specific unit cells and the influence of bulk material properties is mostly negligible. There are many types of auxetic unit cells, characterized by different geometries, auxetic effect and stiffness, and their geometry can be modified to tailor those properties to some extent (Elipe and Lantada 2012; Bhullar 2015; Lim 2015).

Multiscale modeling allows to significantly reduce computational resources requirements of precisely solving problems in which phenomena occurring in different length scales need to be taken into account. In solid mechanics it is used, among others, in analyses of macroscale components manufactured from materials with specific micro- or nano-structures. While material properties of bulk material from which those micro- or nano-structures are known, they are not identical with mechanical properties of those lower scale structures. Hence, first a representative volume element (RVE) of a given structure is modeled and analyzed, its mechanical properties are determined and later are applied as material properties in macroscale analysis (Horstemeyer 2009). One of notable examples of multiscale modeling application is biomechanics and strength analyses of bone tissue (Garcia-Aznar et al. 2021). In scope of this paper, multiscale modeling is used to obtain material properties of selected periodic microstructures based on geometries of their respective unit cells.

A study with the goal to maximize the effective Young's modulus of a two-phase composite material by exploiting the Poisson effect was conducted with success by Long et al. (2016). In this study a three dimensional cube composed of two phases; conventional and auxetic, was considered and distribution of composite phases was optimized in order to maximize the effective Young's modulus of the cube. The values of Poisson's ratio of composite phases were taken arbitrarily and were equal to 0.4 and − 0.9 for conventional and auxetic phases respectively, and the values of Young's modulus were assumed to be equal to 1.0 for both phases and in case of one example the value of Young's modulus of the auxetic phase ranged from 3.0 to 9.0, while for conventional phase it remained at 1.0. While such values might be possible to obtain within the broad spectrum of many known and potential auxetic structures, the authors of this paper wanted to perform a similar study using material properties obtained via multiscale modeling of microstructures based on known auxetic unit cells.

This paper presents the results of development of a hybrid material with auxetic phase, composed of two periodical microstructures, with the goal to maximize the value of effective Young's modulus and, independently, to obtain effective Poisson's ratio equal to 0. Multiscale modeling, FEM simulation and optimization were conducted with the use of Ansys Workbench Mechanical 2023 R1 software.

2 Methods

2.1 Multiscale modeling

Material properties of analyzed phases were determined based on geometries of singular unit cells via multiscale modeling. First, 3D CAD models of microscale unit cells with 1 μm thickness were generated in Autodesk Inventor program. Then, obtained representative volume elements (RVEs) were imported to Material designer environment of Ansys software, which was used to determine the material properties of phases composed of microscale unit cells. 4 unit cells were considered; uniform honeycomb, which served as conventional phase and 3 types of auxetic structures: hex reentrant, 4-vertice star and 2 × 2 "S" cell.

Hex reentrant is one of the most popular auxetic geometries and is widely used in research focusing on auxetic structures in applications of impact energy absorption, some examples include works of Gohar et al. (2021), Wang et al. (2020) and Tan et al. (2021). 4-vertice star is an example of isotropic unit cell and part of a larger "family" of unit cells composed of an orthogonal cross, which arms are connected by compliant geometries, such as tetra-petal geometry considered by Wang et al. (2019) and its many variations. 2 × 2 "S" cell is based on the auxetic structure with reduced stress concentration proposed by Meena and Signamneni (Meena and Singamneni 2019). Both, 4-vertice star and 2 × 2 "S" cell were previously analyzed as individual cells and 5 × 5 structures in regard to auxetic effect in the previous work of the authors (Zawistowski and Poteralski 2023).

Maximum mesh sizes of 0.3 μm were assumed for uniform honeycomb and hex reentrant unit cells, and of 0.15 μm for 4-vertice star and 2 × 2 "S" cell unit cells. ABS polymer from Ansys material database was selected as the bulk material. Analyzed unit cells with dimensions are given in Fig. 1.

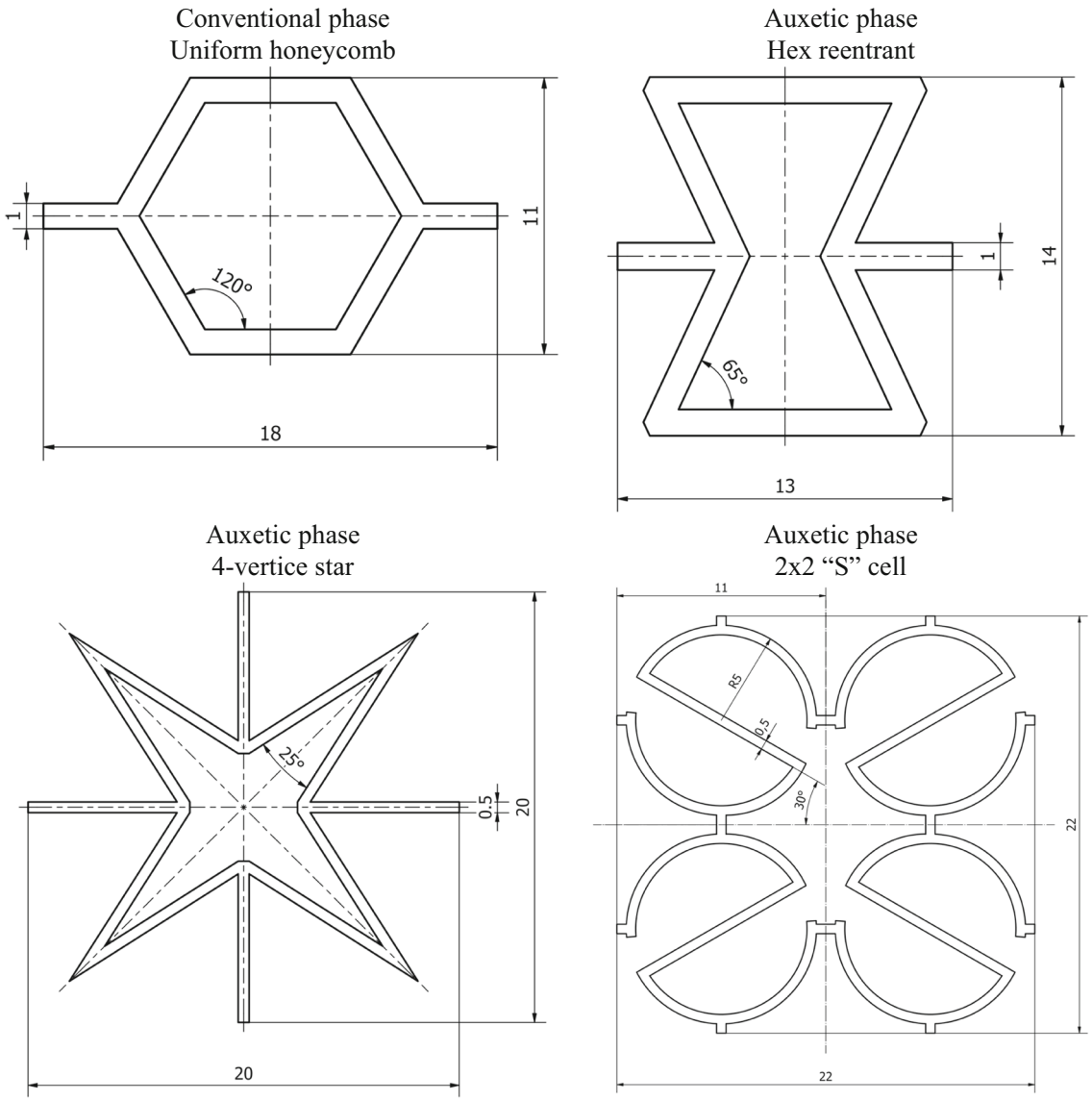

Fig. 1 Dimensions of analyzed unit cells (in μm)

2.2 Hybrid material analysis

Effective Poisson's ratio and Effective Young's modulus of the hybrid material sample were calculated based on the effective strain (proportional deformation) of the sample:

$$\varepsilon_{eff} = \frac{\Delta L_{avg}}{L} \tag{2.1}$$

where ε_{eff} is the effective strain, L is the initial total length of the sample in the considered dimension and ΔL_{avg} is the averaged increment of length in the considered dimension, measured on the sample external edges.

The formula for effective Poisson's ratio is given as follows:

$$\upsilon_{eff} = -\frac{\varepsilon_{Teff}}{\varepsilon_{Aeff}} \tag{2.2}$$

where υ_{eff} is the effective Poisson's ratio, and ε_{Teff} and ε_{Aeff} are the effective strains in transversal and axial directions, respectively.

Effective Young's modulus was determined based on effective strain (2.1) and effective stress:

$$\sigma_{eff} = \frac{P}{A} \tag{2.3}$$

where σ_{eff} is the effective stress, P is the loading force and A is the sample cross-section area. In scope of performed analyses, both P and A were constant and equal to 50 N and 100 mm^2, respectively. Due to this, the effective stress σ_{eff} was also constant, and equal to 0.5 MPa.

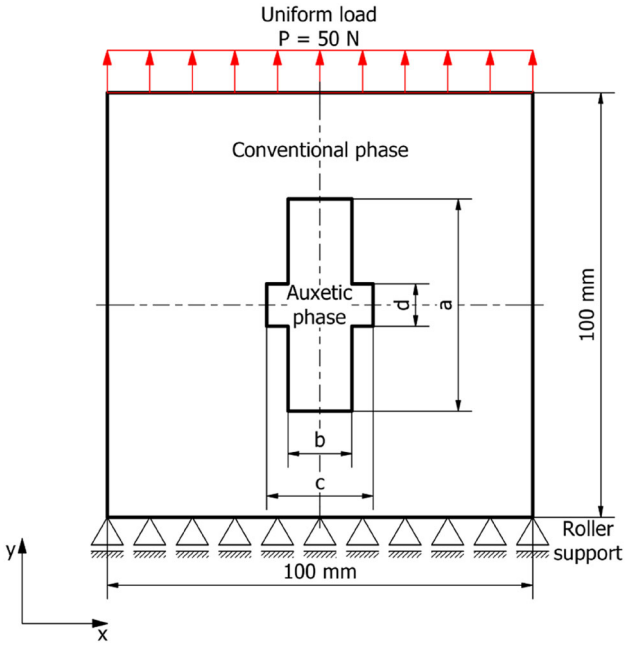

Fig. 2 Sample dimensions and boundary conditions

Table 1 Material properties of ABS polymer

Property	Value
Density ρ [kg/m^3]	1030
Young's modulus E [MPa]	1628
Poisson's ratio ν	0.409

Formula for effective Young's modulus:

$$E_{eff} = \frac{\sigma_{eff}}{\varepsilon_{Aeff}} = \frac{0.5MPa}{\varepsilon_{Aeff}} \tag{2.4}$$

ε_{Aeff} (effective strain in axial direction) is the effective strain in the direction of loading.

The analysis boundary conditions were as follows: a rectangular 2D sample with dimensions 100 × 100 mm with 1 mm thickness was considered, consisting of conventional phase and auxetic phase regions was considered. Auxetic phase region was composed of two intersecting rectangles centered on the sample's middle point. Dimensions of auxetic phase region were parametrized. Roller support was applied to the bottom edge of the sample, while uniform load with magnitude $P = 50$ N was applied to the top edge of the sample. Mesh of uniform quadratic quadrilateral 1 mm finite elements was applied. Analysis boundary conditions are illustrated in Fig. 2.

Assumed material properties of ABS polymer are given in Table 1.

Table 2 Material properties of analyzed phases

Phase type	Conventional phase	Auxetic phase
Unit cell	Uniform honeycomb	Hex reentrant
Geometry	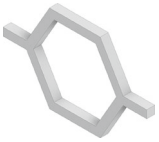	
Density ρ [kg/m^3]	209.27	324.55
Young's modulus E_x [MPa]	18.70	7.49
Young's modulus E_y [MPa]	19.78	40.54
Poisson's ratio ν	0.87	− 0.38
Phase type	Auxetic phase	Auxetic phase
Unit cell	4-vertice star	2 × 2 "S" cell
Geometry		
Density ρ [kg/m3]	124.31	150.85
Young's modulus E_x [MPa]	0.46	0.10
Young's modulus E_y [MPa]	0.46	0.34
Poisson's ratio ν	− 0.57	− 0.39

2.3 Optimization

After initial analysis of auxetic region dimensions' influence on the sample effective Young's modulus and effective Poisson's ratio, simple built-in Ansys optimization tool was applied to obtain the desired variants of hybrid material via parametric optimization. Optimization ranges of geometric parameters were specified based on the results of the initial analysis.

First solution variant was maximization of sample's effective Young's modulus. Objective function was as follows:

$$E_{yeff}(a, b, c, d) \Rightarrow max \tag{2.5}$$

Second solution variant was to obtain zero-value effective Poisson's ratio. Objective function was as follows:

Table 3 Analysis results for selected combinations of auxetic region dimensions and phase types

Phase type	Dimensions of auxetic phase region [mm]				Area percentage of auxetic region [%]	Effective Young's modulus [MPa]	Effective Poisson's ratio
	a	b	c	d			
Reference (honeycomb)	–	–	–	–	0	19.782	0.919
Hex reentrant	30	10	30	10	5	21.280	0.889
Hex reentrant	80	50	80	50	55	35.930	− 0.067
Hex reentrant	90	85	90	85	80.75	45.502	− 1.271
4-vertice star	55	5	10	5	3	19.012	0.893
4-vertice star	60	15	30	10	10.5	18.605	0.859
4-vertice star	40	35	40	35	15.75	13.037	0.694
„S" cell	95	5	10	5	5	18.606	0.870
„S" cell	30	20	30	20	8	15.970	0.805
„S" cell	55	20	55	20	18	10.455	0.699

Table 4 Hybrid material with maximized effective Young's modulus

Phase type	Dimensions of auxetic phase region [mm]				Area percentage of auxetic region [%]	Effective Young's modulus [MPa]	Effective Poisson's ratio
	a	b	c	d			
Hex reentrant	90	51	94	89	85.03	47.90	− 1.48

$$v(a, b, c, d) \Rightarrow 0 \tag{2.6}$$

3 Results

3.1 Material properties of analyzed phases

Material properties of analyzed phases obtained via multiscale modeling in Ansys Material Designer are given in Table 2. There is a considerable difference of stiffness between pairs of uniform honeycomb and hex reentrant cells, and 4-vertice star and 2 × 2 "S" cell. Uniform honeycomb and hex reentrant cells have comparable values of Young's modulus, while for 4-vertice star and 2 × 2 "S" cell those values are lower by two orders of magnitude.

3.2 Hybrid material

Analysis of auxetic region's geometric parameters influence on the sample's effective Young's modulus and Poisson's ratio was performed via series of simulations with incremental increases of a, b, c and d parameters by 5 mm, in the range of 5 to 95 mm, for each type of auxetic phase. It quickly became evident that obtaining increased effective Young's modulus or auxetic behavior of the sample is impossible in case of 4-vertice star and 2 × 2 "S" cells, due to their significantly lower stiffness in comparison to the uniform honeycomb. In case of hex reentrant unit cell, it was possible to obtain both increased effective Young's modulus and negative effective Poisson's ratio, as well as near-zero value of effective Poisson's ratio of the sample. Results for selected combinations of parameters values and phase types are given in Table 3.

3.3 First variant – maximized effective Young's modulus

Optimization range for first hybrid material variant was set based on preliminary analysis results; a, c in the range of [80, 95] mm, b, d in the range of [50, 90] mm. Results are given in Table 4. Comparison of vertical deformation,

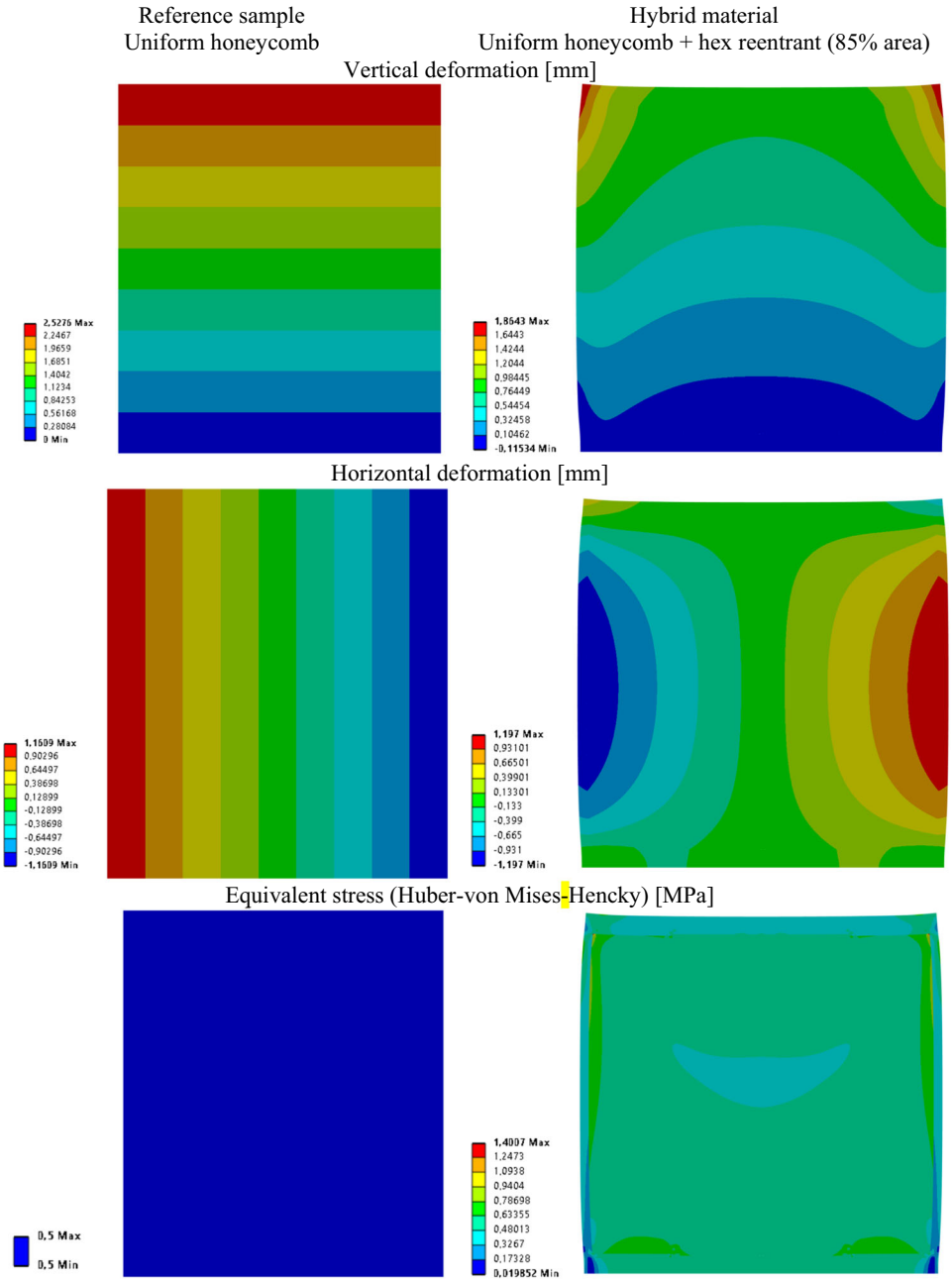

Fig. 3 Comparison of reference sample and hybrid material with maximized Effective Young's modulus

horizontal deformation and equivalent stress distributions in reference sample and hybrid material with maximized effective Young's modulus is given in Fig. 3. A relative increase of 18.15% of effective Young's modulus in relation to hex reentrant phase was obtained.

3.4 Second variant – zero-value effective Poisson's ratio

Optimization range for second hybrid material variant was set based on preliminary analysis results; $a, c = [50, 95]$ mm, $b, d = [5, 50]$ mm. Results are given in Table 5. Comparison

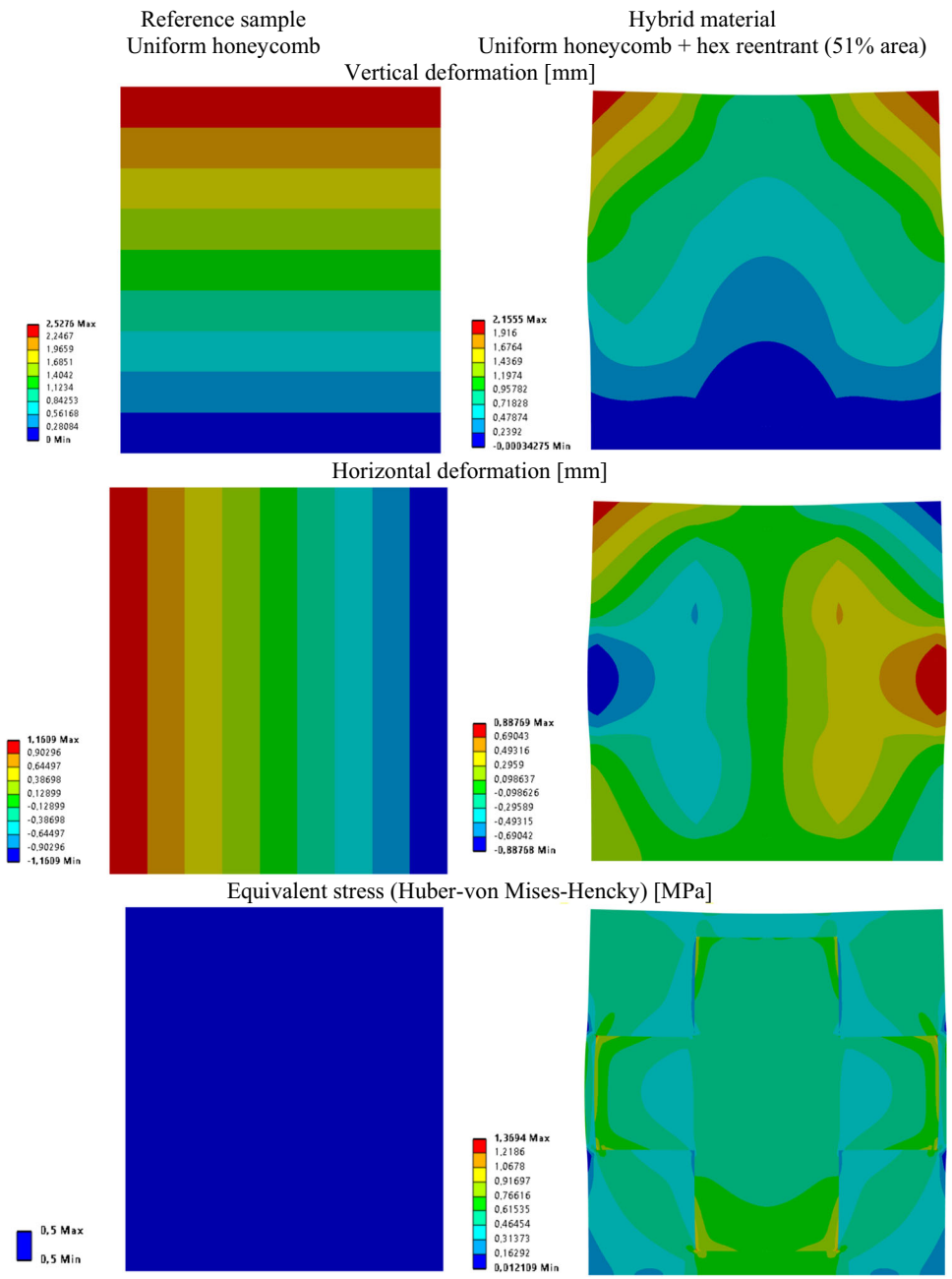

Fig. 4 Comparison of reference sample and hybrid material with zero-value effective Poisson's ratio

Table 5 Hybrid material with zero-value effective Poisson's ratio

Phase type	Dimensions of auxetic phase region [mm]				Area percentage of auxetic region [%]	Effective Young's modulus [MPa]	Effective Poisson's ratio
	a	b	c	d			
Hex reen-trant	87	39	94	31	51.45	34.15	0.003

of vertical deformation, horizontal deformation and equivalent stress distributions in material with maximized effective Young's modulus is given in Fig. 4. Lowest value of effective Poisson's ratio equal to 0.003 was obtained.

4 Summary and conclusions

This paper presents the results of development of a hybrid material with auxetic phase. Performed simulations confirm that it is possible to obtain both a hybrid material with increased effective Young's modulus and a hybrid material with near-zero value Poisson's ratio by combining conventional and auxetic phases with material properties obtained via multiscale modeling, made from the same bulk material. However, it is only possible when stiffnesses of conventional and auxetic phases are comparable. In both solutions variants it was possible to obtain satisfactory results with hex reentrant auxetic phase.

Material properties of analyzed phases obtained via multiscale modeling differ significantly for each microscale unit cell, even though they were all made from the same bulk material (ABS). Differences in effective material properties stem only from geometries of specific unit cells. It is possible to customize and tailor properties of a structure by modifying the geometry of its unit cell. Of course, technological limitations apply and need to be taken into account during design stage of manufacturing.

In first variant an 18.15% increase of effective Young's modulus in relation to the stiffer of compound phases was obtained. Also, effective Poisson's ratio of the sample was equal to − 1.48 which is significantly lower than Poisson's ratios of both compound phases. Effective Poisson's ratios lower than − 1.0 can occur in anisotropic materials, which is the case of both compound phases and the resulting hybrid material.

In second solution variant an effective Poisson's ratio equal to 0.003 was obtained. The value was obtained by taking into account the averaged deformations of sample external edges. As one can observe in Fig. 4, the sample sides did expand laterally in the middle of sample height, and contracted near top and bottom edges. It might be possible to obtain a more uniform deformation distribution also resulting in near-zero effective Poisson's ratio with more complex distribution patterns of auxetic region in the sample.

Obtained results show that in case of auxetic structures application in hybrid materials development, it is important to pay attention not only to their effective Poisson's ratio values, which is the measure of their auxetic effect, but also to their stiffness, which needs to be comparable with stiffnesses of the other phases. As such, one might question the popular development direction of maximizing the auxetic effect and reducing the internal stress of auxetic structures in favor of a less intuitive approach, which would focus on obtaining sufficiently stiff auxetic structures with a wide range of elastic deformation.

Open Access This article is licensed under a Creative Commons Attribution 4.0 International License, which permits use, sharing, adaptation, distribution and reproduction in any medium or format, as long as you give appropriate credit to the original author(s) and the source, provide a link to the Creative Commons licence, and indicate if changes were made. The images or other third party material in this article are included in the article's Creative Commons licence, unless indicated otherwise in a credit line to the material. If material is not included in the article's Creative Commons licence and your intended use is not permitted by statutory regulation or exceeds the permitted use, you will need to obtain permission directly from the copyright holder. To view a copy of this licence, visit http://creativecommons.org/licenses/by/4.0/.

Acknowledgements The research was funded from the projects of Silesian University of Technology, Faculty of Mechanical Engineering.

Author contributions Conceptualization, A.P., M.Z.; Formal analysis, M.Z., A.P.; Simulations, M.Z., A.P.; Verification, Validation and Testing, M.Z., A.P.; Writing—review and editing, M.Z., A.P. All authors have read and agreed to the published version of the manuscript.

Data availability No datasets were generated or analyzed during the current study.

Declarations

Conflict of interest The authors declare no competing interests.

References

Ashby MF, Bréchet YJM (2003) Designing hybrid materials. Acta Mater 51(19):5801–5821

Bhullar SK (2015) Three decades of auxetic polymers: a review. e-Polymers 15(4):205–215

Elipe JCA, Lantada AD (2012) Comparative study of auxetic geometries by means of computer-aided design and engineering. Smart Mater Struct 21:10

Evans KE (1991) Auxetic polymers: a new range of materials. Endeavour 15(4):170–174

García-Aznar JM, Nasello G, Hervas-Raluy S, Pérez MA, Gómez-Benito MJ (2021) Multiscale modeling of bone tissue mechanobiology. Bone 151:116032

Gohar S, Hussain G, Ilyas M, Ali A (2021) Performance of 3D printed topologically optimized novel auxetic structures under compressive loading: experimental and FE analyses. J Market Res 2021(15):394–408

Horstemeyer MF (2009) Multiscale modeling: a review. In: Leszczynski J, Shukla M (eds) Practical aspects of computational chemistry. Springer, Dordrecht

Kromm FX, Quenisset JM, Harry R, Lorriot T (2002) An example of multimaterials design. Adv Eng Mater 4:371–374

Lim TC (2015) Auxetic materials and structures. Springer Science+Business Media, Singapore

Long K, Du X, Xu S, Xie YM (2016) Maximizing the effective Young's modulus of a composite material by exploiting the Poisson effect. Compos Struct 153:596–600

Meena K, Singamneni S (2019) A new auxetic structure with significantly reduced stress concetration effects. Mater Design 173:107779

Momoh EO, Jayasinghe A, Hajsadeghi M, Vinai R, Evans KE, Kripakaran P, Orr J (2024) A state-of-the-art review on the application of auxetic materials in cementitious composites. Thin-Walled Struct 196:111447

Tan H, He Z, Li E, Cheng A, Chen T, Tan X, Li Q, Xu B (2021) Crashworthiness design and multi-objective optimization of a novel auxetic hierarchical honeycomb crash box. Struct Multidiscip Optim 2021(64):2009–2024

Wang ZP et al (2019) Systematic design of tetra-petals auxetic structures with stiffness constraint. Mater Design 170:107669

Wang T, Li Z, Wang L, Hulbert GH (2020) Crashworthiness analysis and collaborative optimization design for a novel crash-box with re-entrant auxetic core. Struct Multidiscip Optim 62:2167–2179

Zawistowski M, Poteralski A (2023) Analysis of geometric parameters influence on lateral strain of selected auxetic elementary cells. Metody Komputerowe 2023:113–116 (**in Polish**)

Publisher's Note Springer Nature remains neutral with regard to jurisdictional claims in published maps and institutional affiliations.